

## Electric field effect in graphite crystallites

Adarsh Sagar, Kannan Balasubramanian, Marko Burghard, and Klaus Kern

Citation: *Appl. Phys. Lett.* **100**, 203116 (2012); doi: 10.1063/1.4719204

View online: <http://dx.doi.org/10.1063/1.4719204>

View Table of Contents: <http://apl.aip.org/resource/1/APPLAB/v100/i20>

Published by the [American Institute of Physics](#).

---

### Related Articles

Surface electrostatic potential transformation of nanodiamond induced by graphitization  
*J. Chem. Phys.* **137**, 154702 (2012)

Surface-plasmon-like modes of graphite powder compact in microwave heating  
*J. Appl. Phys.* **112**, 034905 (2012)

Orientation-dependent friction between a carbon nanotube and graphite  
*Appl. Phys. Lett.* **101**, 063109 (2012)

Laser induced non-thermal deposition of ultrathin graphite  
*Appl. Phys. Lett.* **100**, 151606 (2012)

Phase behavior of mixed submonolayer films of krypton and xenon on graphite  
*J. Chem. Phys.* **136**, 144702 (2012)

---

### Additional information on *Appl. Phys. Lett.*

Journal Homepage: <http://apl.aip.org/>

Journal Information: [http://apl.aip.org/about/about\\_the\\_journal](http://apl.aip.org/about/about_the_journal)

Top downloads: [http://apl.aip.org/features/most\\_downloaded](http://apl.aip.org/features/most_downloaded)

Information for Authors: <http://apl.aip.org/authors>

## ADVERTISEMENT



**ACCELERATE COMPUTATIONAL CHEMISTRY BY 5X.  
TRY IT ON A FREE, REMOTELY-HOSTED CLUSTER.**

[LEARN MORE](#)

## Electric field effect in graphite crystallites

Adarsh Sagar,<sup>1,a)</sup> Kannan Balasubramanian,<sup>1,a)</sup> Marko Burghard,<sup>1</sup> and Klaus Kern<sup>1,2</sup>

<sup>1</sup>Max Planck Institute for Solid State Research, Heisenbergstrasse 1, D-70569 Stuttgart, Germany

<sup>2</sup>Institute de Physique de la Matière Condensée, Ecole Polytechnique Fédérale de Lausanne, EPFL, CH-1015 Lausanne, Switzerland

(Received 20 February 2012; accepted 2 May 2012; published online 17 May 2012)

Graphite is a highly anisotropic crystal with a quasi-two-dimensional electronic structure exhibiting high intrinsic charge carrier mobility. Here, we investigate the effect of an electric field on the resistance of individual graphite crystallites with a thickness on the order of 40 nm. Ambipolar field-effect behavior was achieved with the aid of a polymer electrolyte gate. By optimizing the device geometry, devices with an on/off current ratio of up to 4 and carrier mobilities of around 100 cm<sup>2</sup>/Vs could be attained directly on the crystallites. © 2012 American Institute of Physics. [<http://dx.doi.org/10.1063/1.4719204>]

Carbon-based devices are emerging to play a key role in a number of applications ranging from energy and computing to life sciences.<sup>1–3</sup> In this context, field-effect engineering of exfoliated graphene devices<sup>4</sup> has provided a particularly strong impetus for the exploration of electronic circuits based on *sp*<sup>2</sup>-carbon. A major advantage of graphene-based devices is the possibility of very high carrier mobilities on the order of 10<sup>4</sup> to 10<sup>5</sup> cm<sup>2</sup>/Vs.<sup>5,6</sup> Despite the absence of a band gap, this characteristic renders graphene circuits interesting for high frequency applications.<sup>7</sup> Comparably higher mobilities in the range of 10<sup>6</sup> to 10<sup>7</sup> cm<sup>2</sup>/Vs have been reported for graphite.<sup>8</sup> Graphite has attracted considerable interest since half a century due to its quasi two-dimensional electronic structure,<sup>9</sup> the presence of Dirac fermions,<sup>10</sup> as well as the prediction of the quantum Hall effect.<sup>11</sup> However, it is inherently difficult to turn off the current in a graphite channel by the action of an electrostatic gate, which explains why the use of graphite for device fabrication has been very limited.

Here, we demonstrate an electric field-effect in crystallites of highly oriented pyrolytic graphite (HOPG), by utilizing the large anisotropy in charge transport arising due to their quasi-two-dimensional (quasi-2D) electronic structure.<sup>12,13</sup> We achieve this by steering the charge transport through the uppermost layers of the crystallite and by deploying a polymer electrolyte gate. The observation of a field-effect in graphite complements the well-documented behaviour of field-effect devices comprised of few-layer graphene.<sup>14–16</sup> The direct use of HOPG as a transistor channel is attractive since it would avoid the tedious procedures that are currently necessary for the controlled preparation of graphene devices, such as exfoliation or transfer techniques. As a first step in this direction, we have obtained devices by structuring the surface of graphite crystallites, in a manner analogous to standard complementary metal-oxide-semiconductor (CMOS) technology.

Devices were fabricated by mechanical exfoliation of a HOPG crystal using scotch tape. The obtained crystallites were transferred onto a silicon substrate covered with a

300 nm thick layer of thermal SiO<sub>2</sub>. Optical (see supplementary material Figure S1) and atomic force microscopy (AFM) were employed to locate the crystallites and determine their height. HOPG crystallites with a thickness of around 40 nm were selected for device fabrication. The corresponding Raman spectra (see supplementary material Figure S2) were found to be in accordance with literature reports for HOPG.<sup>17</sup>

In order to electrically address preferably the topmost graphene layer of the crystallites, a SiO<sub>x</sub> insulating layer was deposited at the edges of the crystallite in a first step, as exemplified by the device shown in Figure 1(a). Subsequently, standard electron beam lithography was used to define the electrodes, followed by thermal evaporation of Ti/Au (1/20 nm) and lift-off. The leads 1-2 serve as contacts to the crystallite in such a way that the injection of carriers would take place mostly through the topmost layer (denoted “surface contacting”). For comparison, a second set of electrodes (numbered 3 and 4) was fabricated on the same crystallite without using the insulating layer. The contacts 3-4 touch the ends of the crystallite and serve as source and drain to the entire graphite channel, such that charge carriers are injected into all the sheets of the stack in parallel (denoted “bulk contacting”). For the above device, the room temperature resistances were determined to be ~683 Ω and ~533 Ω for the 1-2 and 3-4 configurations, respectively. The slightly lower resistance observed for the 3-4 combination is likely to originate from two factors. The first one relates to a larger number of graphene layers contributing to the electrical transport, as compared to the 1-2 contact pair. Second, the electrodes 3 and 4 have a comparatively larger contact area with the HOPG surface, which may lead to a lower contact resistance. These assertions gain support from scanning photocurrent microscopy (SPCM) measurements on the same device (see Figures 1(b) and 1(c)). In these experiments, the photocurrent generated upon illumination at zero bias is mapped with a diffraction-limited laser spot.<sup>18–22</sup> For the contacts 1-2, narrow photocurrent lobes can be observed close to the contact edges. On the other hand, in the case of contacts 3-4, the photocurrent signal is laterally much more extended, pointing toward a lower spread resistance of the two contacts in comparison to the 1-2 contact pair. This

<sup>a)</sup>Authors to whom correspondence should be addressed. Electronic addresses: a.sagar@fkf.mpg.de and b.kannan@fkf.mpg.de.

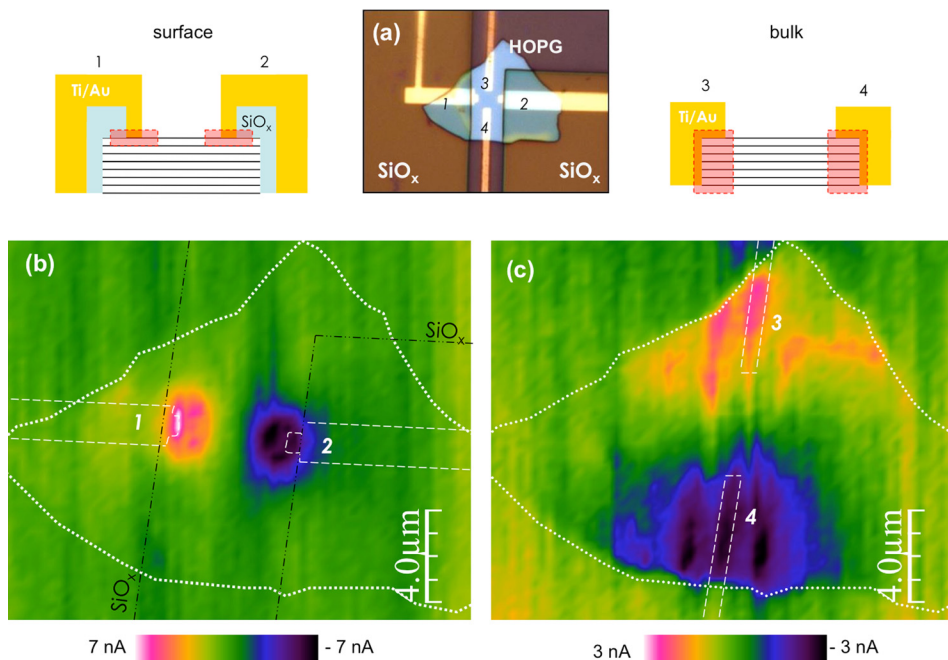


FIG. 1. (a) Optical image of the HOPG crystallite contacted in two different configurations: injection of charge carriers through the surface (1-2) or through the bulk (3-4). (b) and (c) Spatially resolved photocurrent maps of the device at zero bias, when the surface (b: configuration 1-2), and when the bulk (c: configuration 3-4) of the HOPG crystallite are contacted. The dotted line marks the boundary of the crystallite, while the dashed line shows the contacts.

conclusion is further confirmed by the observation of a lower photovoltage (calculated using the respective dark resistance) of  $1.5 \mu\text{V}$  in case of the 3-4 contact pair, as compared to the value of  $4.5 \mu\text{V}$  for the 1-2 configuration.

Upon application of a back gate voltage to the device described above, no field-effect on the graphite channel resistance could be detected for either of the two contact configurations, as illustrated in Figure 2(a). By contrast, with the aid of a polymer electrolyte gate (PEG, Ag wire in a poly(ethyleneoxide)/lithium perchlorate mixture<sup>22</sup>), the resistance could be tuned in both cases (see Figure 2(b)). The possibility to modulate the resistance using the PEG rather than by the back-gate is due to the fact that the gate capacitance in the former case is determined by the electrical double layer (ca. 1 nm), while it is governed by the thickness of the SiO<sub>2</sub> dielectric (300 nm) for the latter. As a result, the gate coupling efficiency is much higher for PEG in comparison to the back-gate.<sup>23</sup> In the PEG configuration, both the transfer curves display a resistance modulation over 1.5% within a small gate voltage range of  $\pm 1.5$  V. This observation suggests that topmost layers in the crystallite are indeed decoupled to an extent sufficient enough to obtain a small field-effect using the polymer electrolyte gate.<sup>16</sup> However, it is somewhat unexpected that the extent of gate action for bulk contacting (3-4) is similar to that of surface contacting (1-2). One plausible explanation for this similarity is the comparatively large channel dimensions for the 3-4 contact pair, which results in a sizeable gate modulation, akin to observations made on back-gated few layer graphene devices.<sup>24</sup> An aspect that distinguishes the two configurations is that for bulk contacting (contacts 3-4) only the *n*-type branch is observed, while the surface-contact configuration (contacts 1-2) exhibits ambipolar behaviour. The shift in the charge neutrality point for the 3-4 contact toward negative gate voltages could be a result of screening produced by the charged upper layers.<sup>16</sup> Defects between adjacent layers and the occurrence of local disorder may also influence the position of the resistance maximum.<sup>25</sup>

The field-effect characteristics of the surface-contacted crystallites could be further improved by geometrically restricting the transport channel to a thin strip between the electrodes. This was done with the aim of focusing the gate impact in a well-defined region between the electrodes. To

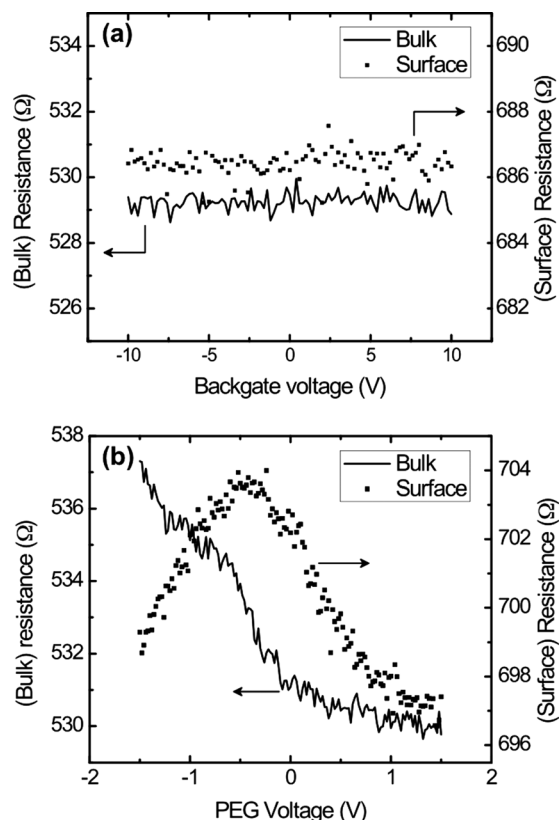


FIG. 2. Gate dependence of resistance for the two contact configurations, namely surface contacts (1-2) and bulk contacts (3-4), using (a) back gate and (b) PEG. In (a), the backgate measurements do not show a field-effect, while in (b), a field-effect can be observed in the same device. The scale for the gate response of the surface contact (1-2) is shown on the right axis while that of the bulk contact (3-4) is shown on the left axis.

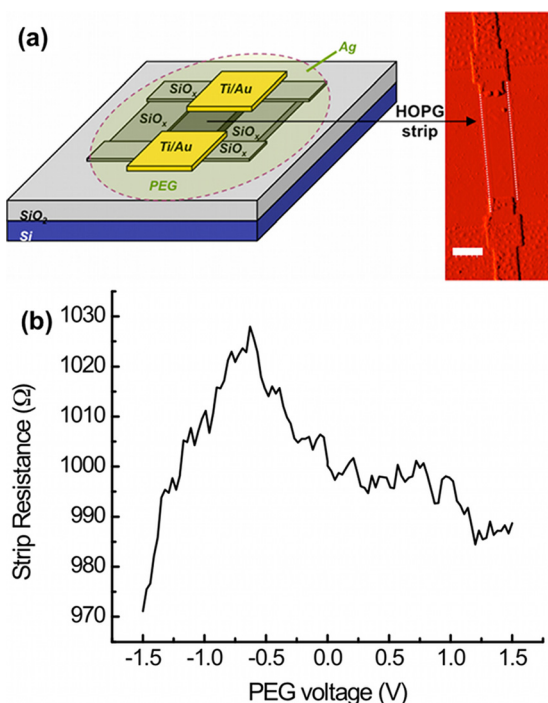


FIG. 3. (a) Device layout showing a schematic of the transistor channel comprising a HOPG strip (AFM image in red) etched out of a graphitic crystallite. The etched regions are passivated with  $\text{SiO}_x$ . The scale bar in the AFM image is 700 nm. (b) Gate dependence of resistance of the etched strip using a PEG showing a resistance modulation of around 10%.

this end, a 700 nm wide strip was fabricated by reactive ion etching with the help of a poly(methyl methacrylate) (PMMA) mask. The non-protected HOPG surface region was then etched using an argon:oxygen flow ratio of 100:11 (sccm) under 0.05 mbars pressure. The etching was carried out for 40 s at a power of 60 W. In order to ensure that the polymer top gate affects only the thin strip, the etched portions of the crystallite were passivated with a  $\sim 40$  nm thick layer of  $\text{SiO}_x$ . A schematic illustration of the final device layout, along with an AFM image of the etched HOPG strip, is presented in Figure 3(a). The transfer curve in Figure 3(b) reveals a resistance modulation of around 10%, and a field-effect mobility of  $245 \text{ cm}^2/\text{Vs}$  can be extracted from the slope of the curve. This corresponds to an improvement in field-effect by one order of magnitude and an increase in field-effect mobility by almost 2 orders of magnitude, in comparison to the device of Figure 1. The slightly different resistance modulation behaviour of this device with respect to that in Figure 2 may arise due to the additional etching step needed for obtaining the graphite strip. Field-effect mobility values on other samples were in the range of  $10^2 \text{ cm}^2/\text{Vs}$ , while a highest gate modulation of around 400% (i.e., an ON/OFF ratio of 4) could be observed in one sample (see supplementary material Figure S3, Ref. 26).

In conclusion, we have demonstrated an ambipolar field-effect in graphite crystallites by engineering the injection of charge carriers into the uppermost layer and by utilizing a polymer electrolyte gate. While as fabricated devices show a low ON/OFF ratio and a field-effect mobility of less

than  $10 \text{ cm}^2/\text{Vs}$ , careful optimization of the contact layout has enabled field-effect mobilities of up to  $100 \text{ cm}^2/\text{Vs}$ . Our configuration has the important advantage that substrate-related effects can be efficiently avoided by the bottom layers,<sup>16</sup> while the gating action takes place in the decoupled upper layers. As a first step toward the direct use of HOPG as a transistor channel, we have obtained devices by structuring the surface of graphite crystallites, in a manner analogous to standard CMOS technology. Further improvements of the device characteristics may be achieved through increased electronic decoupling between the graphene layers, either by the use of intercalating agents or by the direct use of graphite intercalation compounds (GICs).

We acknowledge the support of Benjamin Krauss and Jurgen Smet for support with the Raman Spectroscopy setup. We also thank Thomas Reindl and Marion Hagel for their assistance in the clean room.

- <sup>1</sup>M. S. Mauter and M. Elimelech, *Environ. Sci. Technol.* **42**, 5843 (2008).
- <sup>2</sup>B. S. Harrison and A. Atalaa, *Biomaterials* **28**, 344 (2007).
- <sup>3</sup>T. Rueckes, K. Kim, E. Joselevich, G. Y. Tseng, C.-L. Cheung, and C. M. Lieber, *Science* **289**, 94 (2000).
- <sup>4</sup>F. Chen, J. Xia, D. K. Ferry, and N. Tao, *Nano Lett.* **9**, 2571 (2009).
- <sup>5</sup>R. S. Shishir and D. K. Ferry, *J. Phys.: Condens. Mater.* **21**, 232204 (2009).
- <sup>6</sup>K. I. Bolotina, K. J. Sikesb, Z. Jianga, d. M. Klimac, G. Fudenberga, J. Honec, P. Kima, and H. L. Stormer, *Solid State Commun.* **146**, 351 (2008).
- <sup>7</sup>Y.-M. Lin, C. Dimitrakopoulos, K. A. Jenkins, D. B. Farmer, H.-Y. Chiu, A. Grill, and Ph. Avouris, *Science* **5**, 5966 (2010).
- <sup>8</sup>L. C. Olsen, *Phys. Rev. B* **6**, 4836 (1972).
- <sup>9</sup>E. Abhramas, S. V. Kravchenko, and M. P. Sarachik, *Rev. Mod. Phys.* **73**, 251 (2001).
- <sup>10</sup>Y. Kopelevich, J. H. S. Torres, R. R. da Silva, F. Mrowka, H. Kempa, and P. Esquinazi, *Phys. Rev. Lett.* **90**, 156402 (2003).
- <sup>11</sup>Y. Zheng and T. Ando, *Phys. Rev. B* **65**, 245420 (2002).
- <sup>12</sup>S. Muzushima, *Carbon* **17**, 187 (1979).
- <sup>13</sup>S. Ono, *J. Phys. Soc. Jpn.* **40**, 498 (1976).
- <sup>14</sup>H. Miyazaki, S. Odaka, T. Sato, S. Tanaka, H. Goto, A. Kanda, K. Tsukagoshi, Y. Ootuka, and Y. Aoyagi, *Appl. Phys. Express* **1**, 034007 (2008).
- <sup>15</sup>R. Olac-vaw, H.-C. Kang, H. Karasawa, Y. Miyamoto, H. Handa, H. Fukidome, T. Suemitsu, M. Suemitsu, and T. Otsuji, *Jpn. J. Appl. Phys.* **49**, 06GG01 (2010).
- <sup>16</sup>Y. Sui and J. Appenzeller, *Nano Lett.* **9**, 2973 (2009).
- <sup>17</sup>S. Reich and C. Thomsen, *Philos. Trans. R. Soc. London, Ser. A* **362**, 2271 (2004).
- <sup>18</sup>K. Balasubramanian, Y. Fan, M. Burghard, K. Kern, M. Friedrich, U. Wannek, and A. Mews, *Appl. Phys. Lett.* **84**, 2400 (2004).
- <sup>19</sup>E. J. H. Lee, K. Balasubramanian, N. Fu, J. Dorfmueller, R. Vogelgesang, A. Mews, M. Burghard, and K. Kern, *Small* **3**, 2038 (2007).
- <sup>20</sup>E. J. H. Lee, K. Balasubramanian, R. T. Weitz, M. Burghard, and K. Kern, *Nat. Nanotechnol.* **3**, 486 (2008).
- <sup>21</sup>F. Xia, T. Mueller, R. Golizadeh-Mojarad, M. Freitag, Y. Lin, J. Tsang, V. Perebeinos, and P. Avouris, *Nano Lett.* **9**, 1039 (2009).
- <sup>22</sup>A. Sagar, E. J. H. Lee, K. Balasubramanian, M. Burghard, and K. Kern, *Nano Lett.* **9**, 3124 (2009).
- <sup>23</sup>A. Das, S. Pisana, B. Chakraborty, S. Piscanec, S. K. Saha, U. V. Waghmare, K. S. Novoselov, H. R. Krishnamurthy, A. K. Geim, A. C. Ferrari, and A. K. Sood, *Nat. Nanotechnol.* **3**, 210 (2008).
- <sup>24</sup>T. Maassen, F. K. Dejene, M. H. D. Guimaraes, C. Józsa, and B. J. van Wees, *Phys. Rev. B* **83**, 115410 (2011).
- <sup>25</sup>Y. Lu, M. Muñoz, C. S. Steplecaru, C. Hao, M. Bai, N. Garcia, K. Schindler, and P. Esquinazi, *Phys. Rev. Lett.* **97**, 076805 (2006).
- <sup>26</sup>See supplementary material at <http://dx.doi.org/10.1063/1.4719204> for optical images and Raman spectra of crystallites, and the field-effect response of an etched strip with high gate modulation.